AFRL-ML-WP-TP-2006-408

EVALUATION AND IMPROVEMENT IN SENSOR PERFORMANCE AND DURABILITY FOR STRUCTURAL HEALTH MONITORING SYSTEMS (PREPRINT)

James L. Blackshire and Adam Cooney

FEBRUARY 2006

Approved for public release; distribution is unlimited.

STINFO FINAL REPORT

MATERIALS AND MANUFACTURING DIRECTORATE
AIR FORCE RESEARCH LABORATORY
AIR FORCE MATERIEL COMMAND
WRIGHT-PATTERSON AIR FORCE BASE, OH 45433-7750

NOTICE

PAO Case Number: AFRL/WS-06-0356, 09 February 2006

THIS TECHNICAL REPORT IS APPROVED FOR PUBLICATION.

/s/

JAMES L. BLACKSHIRE
Research Engineer
Nondestructive Evaluation Branch
Metals, Ceramics and NDE Division

/s/

THOMAS J MORAN
Technology Development Leader
Nondestructive Evaluation Branch
Metals, Ceramics and NDE Division

/s/

GERALD J. PETRAK, Asst. Chief
Metals, Ceramics and NDE Division
Manufacturing Technology Directorate

REPORT DOCUMENTATION PAGE

Form Approved OMB No. 0704-0188

1. REPORT DATE *(DD-MM-YY)*
February 2006

2. REPORT TYPE
Conference Paper Preprint

3. DATES COVERED *(From - To)*

4. TITLE AND SUBTITLE
EVALUATION AND IMPROVEMENT IN SENSOR PERFORMANCE AND DURABILITY FOR STRUCTURAL HEALTH MONITORING SYSTEMS (Preprint)

5a. CONTRACT NUMBER
In-House

5b. GRANT NUMBER

5c. PROGRAM ELEMENT NUMBER
N/A

5d. PROJECT NUMBER
N/A

5e. TASK NUMBER
N/A

5f. WORK UNIT NUMBER
N/A

6. AUTHOR(S)
James L. Blackshire and Adam Cooney (AFRL/MLLP)

7. PERFORMING ORGANIZATION NAME(S) AND ADDRESS(ES)
Nondestructive Evaluation Branch (AFRL/MLLP)
Metals, Ceramics and NDE Division
Materials and Manufacturing Directorate
Air Force Research Laboratory, Air Force Materiel Command
Wright-Patterson AFB, OH 45433-7750

8. PERFORMING ORGANIZATION REPORT NUMBER
AFRL-ML-WP-TP-2006-408

9. SPONSORING/MONITORING AGENCY NAME(S) AND ADDRESS(ES)
Materials and Manufacturing Directorate
Air Force Research Laboratory
Air Force Materiel Command
Wright-Patterson AFB, OH 45433-7750

10. SPONSORING/MONITORING AGENCY ACRONYM(S)
AFRL-ML-WP

11. SPONSORING/MONITORING AGENCY REPORT NUMBER(S)
AFRL-ML-WP-TP-2006-408

12. DISTRIBUTION/AVAILABILITY STATEMENT
Approved for public release; distribution is unlimited.

13. SUPPLEMENTARY NOTES
Report contains color. This work has been submitted for publication in proceedings of the Conference on Advanced Sensor Technologies in Nondestructive Evaluation and Structural Health Monitoring, SPIE.

14. ABSTRACT

This paper describes the evaluation of the long-term durability and performance of surface-bonded piezo sensors for detecting cracks and corrosion in aerospace materials. The technology is mature and widely known throughout the scientific community.

15. SUBJECT TERMS
Structural Health Monitoring, Piezo Wafer Active Sensors, Displacement-Field Imaging

16. SECURITY CLASSIFICATION OF: a. REPORT	b. ABSTRACT	c. THIS PAGE	17. LIMITATION OF ABSTRACT:	18. NUMBER OF PAGES	19a. NAME OF RESPONSIBLE PERSON (Monitor)
Unclassified	Unclassified	Unclassified	SAR	16	James Blackshire **19b. TELEPHONE NUMBER** *(Include Area Code)* (937) 255-9802

Standard Form 298 (Rev. 8-98)
Prescribed by ANSI Std. Z39-18

Evaluation and Improvement in Sensor Performance and Durability for Structural Health Monitoring Systems

James L. Blackshire and Adam Cooney

Air Force Research Lab (AFRL/MLLP)
Wright-Patterson AFB, OH 45433

ABSTRACT

For aerospace applications, the successful transition and use of integrated structural health monitoring systems will require durable sensors that can perform in their intended environment for many years. For legacy aircraft the primary means of implementing a sensor system will be through surface mounting or bonding of the sensors to the structure. Previous work has shown that the performance of surface-bonded piezo sensors can degrade due to environmental effects such as vibrations, temperature fluctuations, and substrate flexure motions. This performance degradation included sensor cracking, disbonding, and general loss of efficiency over time. In this activity, the bond and piezo material characteristics of a typical surface-bonded piezo sensor system were studied to understand and improve the long-term durability and survivability of the sensor system. Analytic and computational models were developed and used to understand stress-strain relationships for the bonded sensor system, with a special emphasis being place on coefficient of thermal expansion issues. Accelerated environmental testing was accomplished for simple bonded piezo sensor systems, where a displacement-field imaging technique was used to understand the piezo sensor performance. Future activities will focus on identifying the optimal bond conditions and piezo material type, with the ultimate goal of improving the robustness of health monitoring systems through improved sensor system design and packaging.

Keywords: Structural Health Monitoring, Bonded Sensors, Displacement-Field Imaging

1. INTRODUCTION

A significant amount of interest currently exists in the area of integrated systems health management (ISHM). Although this basic concept can take on many different functional forms, for aerospace systems the use of structural health monitoring (SHM) as part of a larger ISHM strategy offers the potential for monitoring the structural health of an aircraft system with far-reaching consequences and benefits [1]. Improved fleet management using condition-based maintenance (CBM) strategies, for example, would use ISHM and SHM to provide critical diagnostic information for assessing the health of the aircraft systems. In a condition-based maintenance framework, aircraft would be maintained more efficiently and effectively using critical health status indicators, which would be provided by an integrated health diagnostic system.

A critical aspect of the ISHM and SHM concepts involves the use of integrated sensing systems to interrogate, inspect, and diagnose the aircraft structure. In practice, the inspection system uses distributed sensors which can be bonded to an existing structure, or integrated directly within a newly fabricated structure [2,3]. In either case, the integrated sensors become a part of the structure, and are therefore subjected to similar or identical environmental conditions. This places additional requirements on the performance of the sensor system with regard to long term durability, survivability, and operation performance over extended time periods, and in a wide variety of varying environmental conditions. These environmental conditions would likely include variations in weather, moisture, chemical attack, vibration, temperature, and mechanical loading of the structural members of the airframe [4]. In addition, the sensors will need to behave in a consistent and reliable manner throughout the duration of the inspection process, which for aerospace structures can span several years and even decades.

This work has been submitted for publication in proceedings of the Conference on Advanced Sensor Technologies in Nondestructive Evaluation and Structural Health Monitoring, SPIE.

Previous work [5-7] has shown that the performance of a surface-bonded piezoelectric sensor can degrade due to environmental stresses, resulting in undesired sensor disbond and cracking events. In this effort, a basic analysis of the stress-strain relationships for a bonded sensor system is provided, with a special emphasis being placed on coefficient of thermal expansion mismatch issues. The analysis first considers the stresses induced in an adhesively bonded sensor from a biaxial stress field in the underlying substrate. In particular, the load transfer mechanism from the substrate through the adhesive layer into the sensor is analyzed. The key result of this analysis describes the partitioning of load between the substrate and sensor as being dependent on the relative stiffness between the two materials. Regarding the influence of the adhesive material layer, the load is found to be asymptotically transferred into the sensor from its edge interface, moving toward the center of the sensor at a rate determined by the shear modulus and thickness of the adhesive, the substrate stiffness, and the sensor thickness. The analysis then continues to include a basic treatment of the stress-strain conditions induced in a bonded sensor by coefficient of thermal expansion (CTE) mismatch between the substrate material and the sensor. For a thin piezoelectric disk bonded to an aluminum panel substrate material, the analysis showed that thermal expansion and contraction of the piezo disk due to modest aircraft temperature cycling events can induce loads approaching nominal failure limits. These preliminary analytic results tend to support the previous experimental evidence for bonded sensor disbond and cracking events, and offer insight into the material properties and load transfer mechanisms which must be considered in durable surface bonded sensor applications. Future activities will focus on identifying the optimal bond conditions and piezo material type, with the ultimate goal of improving the robustness of health monitoring systems through improved sensor system design and packaging.

2. SURFACE-BONDED SENSOR DURABILITY STUDIES

A critical aspect of ISHM and SHM system development involves the long-term stability and durability of the integrated sensors. For surface-bonded sensors in an aircraft environment, the dynamic loading of the airframe needs to be considered and addressed for its effect on the sensor system. Stresses in the bonded sensors can be induced by mechanical loading, bending, and thermally induced stresses of the substrate. Biaxial and bending stresses in the substrate, for example, can result from externally applied loads or naturally occurring vibrations within the structure. The thermally induced stresses can arise from differences in the thermal coefficient of expansion between the substrate and sensor material. In all cases, sensor load-carrying strength limits may be approached or exceeded leading to bond-failure or sensor damage.

Previous integrated sensor durability studies have shown potential problems with regard to the durability and long-term performance of surface bonded piezoelectric sensors [5-7]. Piezoelectric materials are naturally brittle in nature, and therefore require special care with regard to understanding their performance features and potential failure modes and damage mechanisms. Figure 1 shows evidence of sensor cracking and sensor disbond in surface bonded piezo disks attached to a thin aluminum panel. The measurements results depicted in Figure 1 were obtained using a noncontact displacement-field imaging technique [8,9], which provides a measure of the out-of-plane motions for the piezoelectric disks as gray-level images. The crack and disbond locations appear as bright regions in the images, which indicates larger motion levels in those locations. The crack is easily imaged due to near-field ultrasound and free-boundary motion effects, while the disbonds are imaged as modal vibration lobe patterns again due to free-boundary motion effects in the disbond region.

a) b)

Fig. 1. Displacement-field images of a) cracked piezoelectric sensor disk, and b) disbonded piezoelectric sensor disk.

In the sensor cracking case (Figure 1a), the sensor was damaged during the installation process due to uneven pressure being applied to the sensor during the bond procedure. In the sensor disbond case (Figure 1b) , the sensor was not fully bonded across its entire surface, again due to inadequate uniform pressure being applied to the sensor during its application to the substrate material surface. In both cases depicted in Figure 1, edge-disbond effects can also be seen around the entire perimeter of both piezo disks, again produced from inadequate pressure being applied in the bond installation process in those regions of the piezo disk material.

Figure 2 provides further evidence of the effects of a damaged piezoelectric sensor disk on its performance level. Figure 2a provides a displacement-field image of a newly-bonded piezoelectric sensor disk that is behaving properly and performing well. The piezo disk is vibrating with a peak displacement level of ~37 nm and is transmitting guided waves into the aluminum substrate material with a displacement level of ~25 nm at a radial distance of 1cm from the piezo sensor edge. The undamaged sensor is seen to have a circularly symmetric displacement pattern within the piezo and external to the sensor position as the elastic wave energy propagates away from the sensor position. Figures 2c-g depict plots of the actual displacement levels at discrete point taken 1 cm radial distance away from sensor perimeter. The drive signal for the transducer was a 1-cycle, 100kHz toneburst signal with a drive voltage of 10Vpp. The output displacement signals depicted in Figures 2c-f show a nominal 1-cycle elastic wave propagating within the aluminum substrate material. Figure 2g depicts a polar plot of the peak displacement levels measured at 12 angular positions (30 degree steps) away from the piezo sensor (1cm radial distance). The angular pattern is seen to be elliptically-shaped, but provides a nominally uniform distribution of energy propagating in all directions away from the piezo disk.

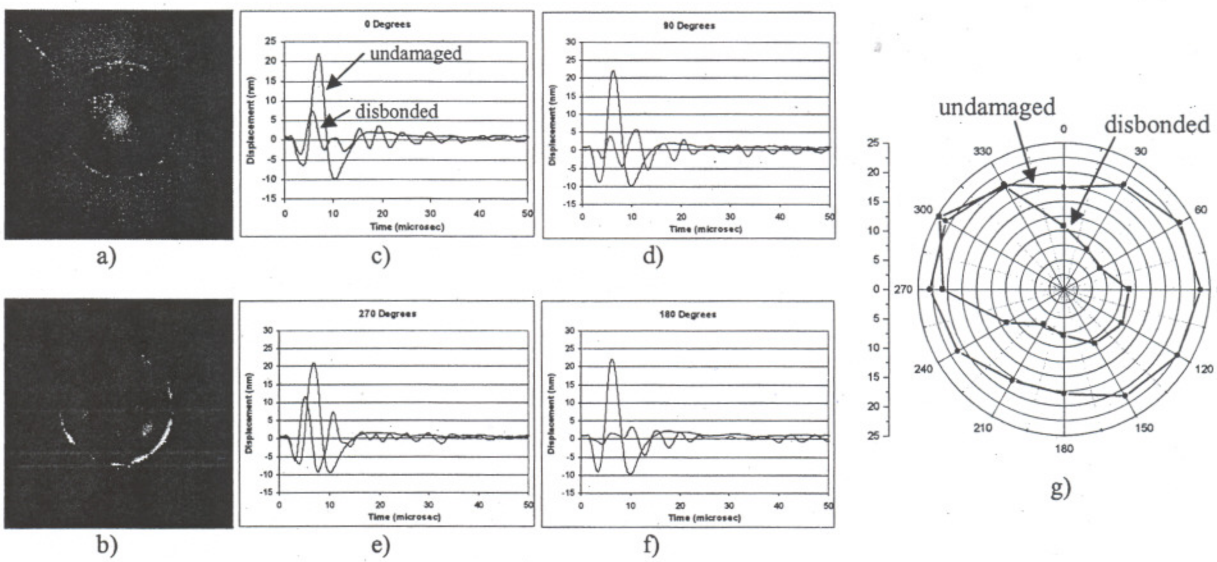

Fig. 2. a) Displacement-field image of undamaged sensor, b) displacement-field image of disbonded sensor after 20 cycles of elevated heat exposure at 175F, c-f) displacement levels versus time measured at 1cm distance from the edge of the sensor for 0°, 90°, 180°, and 270° angular directions, and g) polar plot of peak displacement levels from 0°-360° at 1cm radial distance from sensor.

Figure 2b depicts a displacement-field image of the same piezo disk after 20 cycles of elevated heat exposure at 175F. The image provides dramatic evidence of a major disbond event. The resulting displacement levels within the piezo disk region have been replaced with structured lobe features, rather than a uniform Bessel-type displacement pattern in the undamaged case. As depicted in Figures 2c-g, the primary effect on the signal generation capability is a drop in efficiency of over 50-80%. In addition, the modal vibration effects within the piezo disk convert the 1-cycle toneburst signal into a multi-cycle, multi-frequency signal that would tend to complicate the damage sensing process. In effect, if this damaged sensor was being used as a generation source, a receiving piezo sensor unit would pick up a complicated waveform signal, which may be misinterpreted as a damage event. The polar plot in Figure 2g also depicts an additional adverse affect of the sensor damage which involves a preferential, redistribution and redirection of propagating energy

in specific directions, and limited/reduced energy propagation in other angular directions. This would tend to reduce damage detection sensitivity levels in certain directions within the substrate material.

The results depicted in Figures 1 and 2 represent damage to the piezo sensor disk in the forms of cracking and disbond. In the cases depicted in Figure 1, the damage was induced by mechanical stress-strain in the form of pressure variations across the disk during the bond installation process. In the case depicted in Figure 2, the disbond event was initiated and grown due to cyclic heat exposures at a moderate elevated temperature level of 175F. This represents one type of environmentally-induced damage that can be expected in an operational aircraft. Another type of sensor degradation has been reported [5,6], which can result in a nominal drop in performance with repeated temperature cycling events. The major results of this study are provided in Figure 3. Figures 3a-c provide measurement results for a freeze-thaw study, while Figures 3d-f provide results for an elevated temperature study. The bonded piezo disks in these studies were subjected to a +/-100F temperature cycling condition relative to a nominal 75F operational temperature. As shown in the figures, a relatively gradual and systematic reduction in the output displacement levels of the piezo transducer disks was observed for both reduced and elevated temperature levels expected in a typical aircraft environment. In both cases, the reduction in output performance followed an approximate quadratic relationship with a leveling off at increasing cycles. The elevated heat exposures showed a more dramatic reduction vs. exposure number, but both cold and hot exposures levels appeared to level off at ~50% of their original levels.

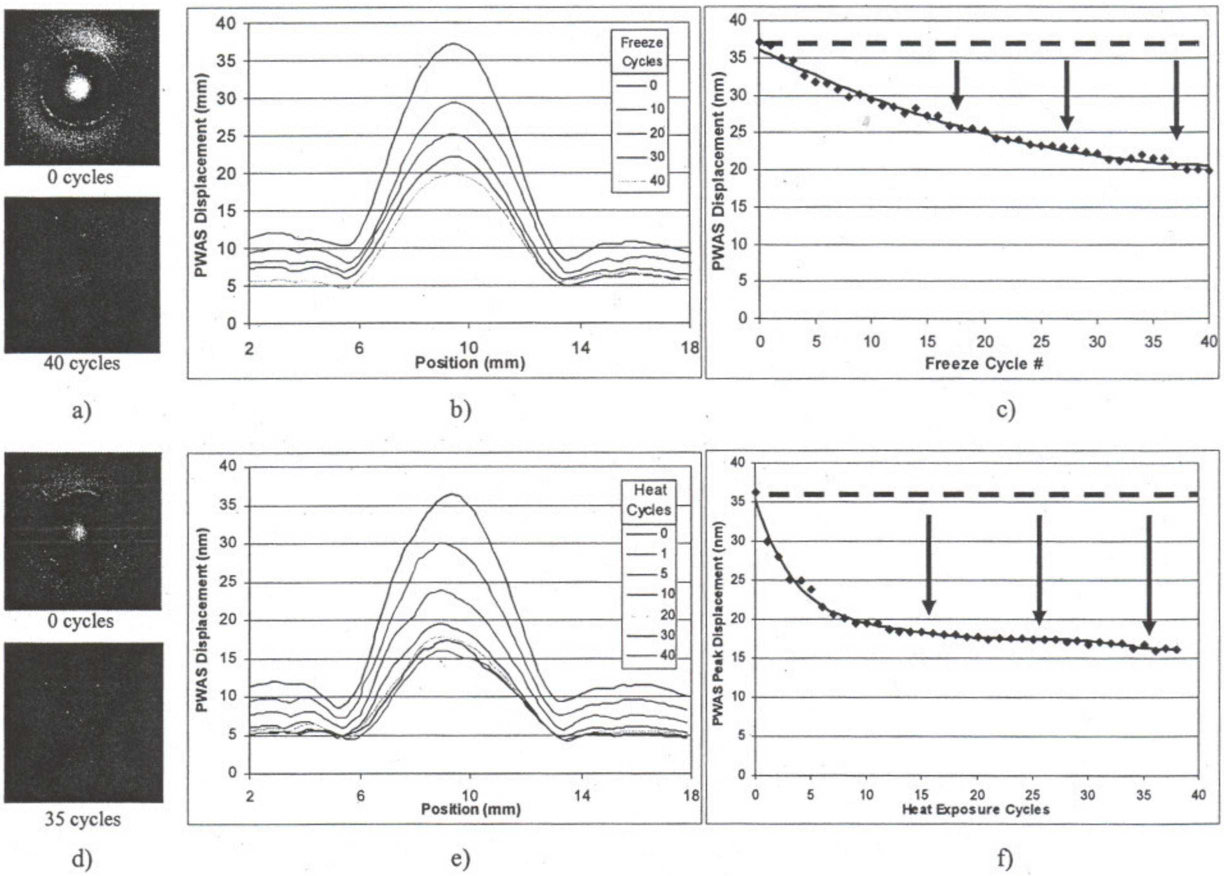

Fig. 3. a) Displacement-field images of sensor disk used in freeze-thaw studies, b) cross-sectional cuts of displacement levels through the center of the piezo disk for increasing number of freeze-thaw cycles, c) peak displacement levels of piezo disk at increasing number of freeze-thaw cycles, d) displacement-field images of sensor disk used in elevated heat studies, b) cross-sectional cuts of displacement levels through center of piezo disk for increasing heating cycles, c) peak displacement levels of piezo disk at increasing number of heat cycles.

3. BASIC STRESS ANALYSIS FOR BONDED PIEZOELECTRIC SENSORS

The experimental results presented in Section 2 provide evidence that surface-bonded sensors can be subjected to conditions in a typical aircraft environment which can result in sensor performance reductions or physical damage to the sensor system. A key player in several of the damage and performance degradation mechanisms for a bonded sensor system involve stress-strain conditions existing within the sensor or the bond. Stresses in bonded sensors are induced by biaxial loading, bending, and thermally induced stresses of the substrate. Biaxial and bending stresses in the substrate result from externally applied loadings, while thermally induced stresses arise from differences in the thermal coefficient of expansion between the substrate and sensor material.

The bonding of the sensor to the substrate determines the effectiveness with which the load is transferred into the sensor. The load transfer mechanism between members in a bonded joint can be explained using the one-dimensional theory of bonded joints [10]. The load transfer is considered to arise as from a shear loading through the adhesive layer as shown in Figure 4. In this theory, each adherent is treated as a one-dimensional continuum with a corresponding Modulus of Elasticity, E, and thickness, t. The adherent deformation is given by a longitudinal displacement, u, and a corresponding longitudinal stress, σ. The stress-displacement relation for a member is:

$$\sigma(y) = Eu'(y) = F/t \tag{1}$$

where F is the load per unit length and differentiation is indicated by the dash('). The adhesive layer acts as a shear spring with the relationship for the adhesive shear stress given by:

$$\tau_a(y) = G_a\gamma_a = (G_a/t_a)[u1(y) - u2(y)] \tag{2}$$

where G_a is the adhesive shear modulus, γ_a is the adhesive shear strain, and t_a is the adhesive layer thickness.

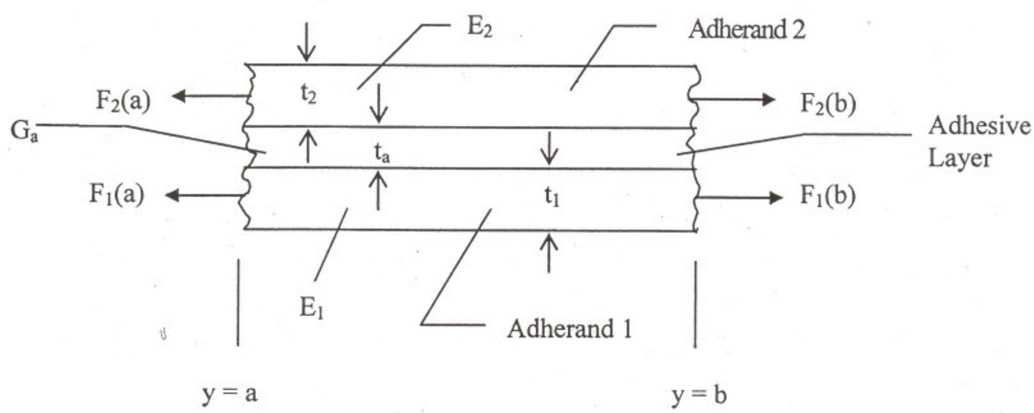

Fig. 4. Segment of an adhesively bonded joint.

The shear tractions exerted by the adhesive can be replaced by an equivalent body force distributed uniformly across the thickness of each adherent, leading to the differential equilibrium equations:

$$t_p\sigma'_p = -t_r\sigma'_r(y) = \tau_a(y). \tag{3}$$

The forgoing assumptions lead to the differential equation:

$$\tau''_a(y) - \beta^2\tau_a(y) = 0 \tag{4}$$

$$\beta^2 = (G_a/t_a)\{(1/E_pt_p) + (1/E_rt_r)\} \tag{5}$$

The general solution for this case is:

$$\tau_a(y) = Ae^{\beta y} + Be^{-\beta y} = 2A\cosh(\beta y) + (B-A)e^{-\beta y} \tag{6}$$

By applying the appropriate boundary conditions, the case for an adhesively bonded sensor can be obtained. The solution for this problem is found over the domain $(-L <= y <= L)$. The equation for β^2 is:

$$\beta^2 = (G_a/t_a)\{(1/E_p t_p) + (1/E_r t_r)\}. \tag{7}$$

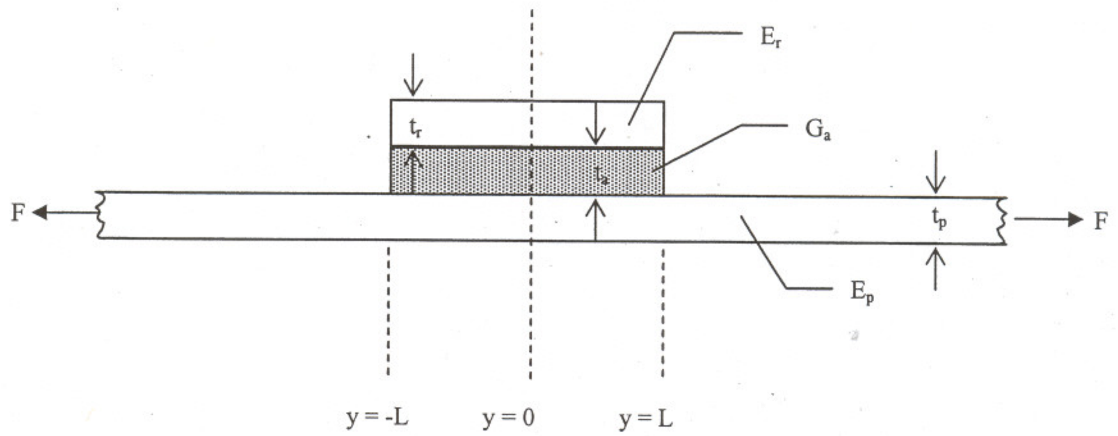

Fig. 5. Adhesively bonded reinforced plate geometry.

The boundary conditions for this problem are:

$$\tau'_a(-L) = (G_a/t_a)\{(\sigma_p(0)/E_p) - (\sigma_r(0)/E_r)\} = (G_a/t_a)\{(F/E_p t_p) - 0\} \tag{8}$$

$$\tau'_a(L) = (G_a/t_a)\{(\sigma_p(L)/E_p) - (\sigma_r(L)/E_r)\} = (G_a/t_a)\{(F/E_p t_p) - 0\}. \tag{9}$$

Using the boundary conditions, the constants for the solution to this problem are:

$$B = -A \tag{10}$$

$$A = (F/E_p t_p))\,(G_a/t_a)(1/2\,\beta\cosh(\beta L)). \tag{11}$$

The relations between the derivatives of the normal stresses and the shear stress are again integrated to give:

$$\sigma_p(y) = \sigma_p(-L) + (1/\beta t_p)\,\{\,2A(\cosh(\beta y) - \cosh(-\beta L))\} =$$

$$\sigma_r(y) = \sigma_r(-L) + (1/\beta t_r)\,\{-2A(\cosh(\beta y) - \cosh(-\beta L))\} \tag{12}$$

$$= (F/E_p t_p))\,(G_a/t_a)\,(1/\beta^2 t_r \cosh(\beta L)))((\cosh(\beta y) - \cosh(-\beta L)))$$

The load is asymptotically transferred into the sensor and approaches a value determined by stiffness partitioning between the sensor and the substrate. This stiffness partitioning value is found from:

$$\sigma_r(sp) = FS/((1+S)t_r) \tag{13}$$

where S is the stiffness ratio defined by:

$$S = (E_r t_r / E_p t_p). \tag{14}$$

The reinforcement stress can be expressed in terms of the stiffness ratio as:

$$\sigma_r(y) = [FS/((1+S)t_r)][\,1 - \{\cosh(\beta y)/\cosh(\beta L)\}] = \sigma_r(sp)[\,1 - \{\cosh(\beta y)/\cosh(\beta L)\}]. \tag{15}$$

The maximum stress value in the reinforcement is at the center, $(y=0)$, and this is:

$$\sigma_r(0) = \sigma_r(sp)[\,1 - \{1/\cosh(\beta L)\}]. \tag{16}$$

It is also observed that:

$$\lim_{\beta L \to \infty} \sigma_r(0) = \sigma_r(sp) \tag{17}$$

and that:

$$\lim_{\beta L \to 0} \sigma_r(0) = 0. \tag{18}$$

Thus, to lower the stress transfer to the reinforcement, the size of the reinforcement or adhesive shear modulus must be decreased or the adhesive layer thickness must be increased. Decreasing the stiffness ratio will also decrease the stress transfer. If the shear modulus becomes infinite or the adhesive layer thickness becomes infinitesimal then the reinforcement stress distribution becomes:

$$\sigma_r(y) = [FS/((1+S)t_r)][H(y+L) - H(y-L)] \tag{19}$$

and the shear stress distribution becomes:

$$\tau_a(y) = -t_r \sigma'_r(y) = -[FS/((1+S))][\,\delta(y+L) - \delta(y-L)]. \tag{20}$$

Using Equation (15), the reinforcement stress for compliant, rigid, and infinitely rigid bonds are shown in Figure 6a, with parameters of: $Ep = 7.31 \times 10^{10}$ Pa, $Er = 8.40 \times 10^{10}$ Pa, $Ga =$ (7.00×10^{6} Pa for compliant, 7.00×10^{8} Pa for rigid, and Infinite), $tp = .001$ m, $tr = 0.0001$ m, $ta = 0.0001$ m, $L = .005$m. Using Equation (20), the adhesive shear stress for a compliant and rigid bond is shown in Figure 6b. From Figure 6, it is clear that the use of a compliant bond helps both with load/stress transfer to the sensor and also with shear stress levels in the bond material layer, which would help with sensor durability and bond integrity issues.

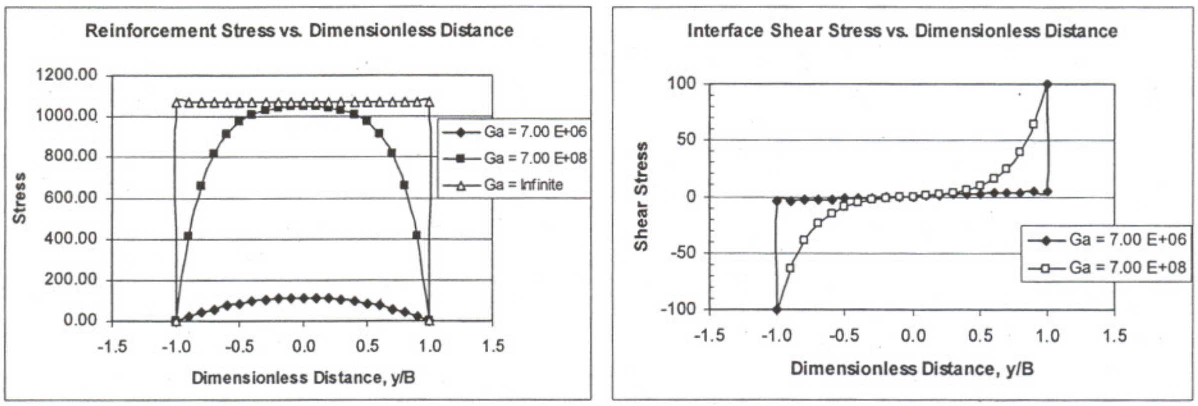

a) b)

Fig. 6. a) Reinforcement stress distribution for 1.0 N/m unit lineal load in a reinforced plate with a compliant, rigid, and infinitely rigid bond, and b) Interface shear stress distribution for 1.0 N/m unit lineal load in a reinforced plate with a compliant and rigid bond.

4. THERMAL EXPANSION/CONTRACTION STRESSES

The expansion of a heated solid can be measured by a quantity α, the coefficient of thermal expansion. This coefficient is defined in such a way that it measures the percentage change in the length/volume per degree temperature change, and can be described in 1-dimensional form as

$$\alpha = \frac{\Delta L / L_o}{\Delta T} \quad , \qquad \Delta L = L_o \alpha \Delta T \quad , \qquad L = L_o(1 + \alpha \Delta T) \tag{21}$$

where L_o is the original length of the material, ΔL is the change in length due to temperature change ΔT. For solid materials, the coefficient of thermal expansion is positive, which means that the solid will expand on heating, and contract on cooling. Figure 7 provides an schematic diagram example of the expansion of a piezoelectric sensor material bonded to an aluminum substrate material due to an increase in temperature. For coefficient of thermal expansion values of $4\text{x}10^{-6}$/°C and $23\text{x}10^{-6}$/°C for the piezoelectric and aluminum materials, respectively, a thermal expansion of 22.5μ/m and 131μ/m is expected for the two materials for a +100F (+55.5C) increase in temperature. This 5-fold difference in expansion levels results in compressive stresses in the substrate material and tensile stresses in the piezoelectric sensor.

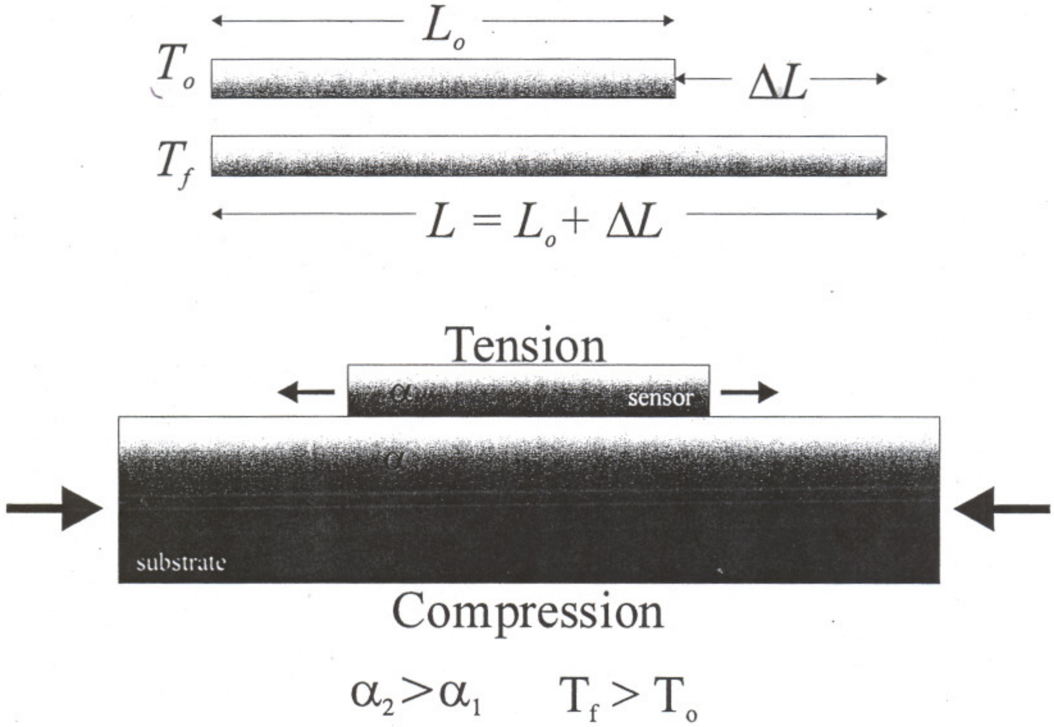

Fig. 7. Expansion of solid materials due to addition of heat energy for bonded sensor on substrate material, resulting in compressive stress in substrate material and tensile stress in sensor.

In order to determine stress levels within the piezoelectric material, the one-dimensional differential thermal expansion depicted in Figure 7 can be treated as an equivalent spring problem. The initial (unloaded) spring heights correspond to the lengths of the piezoelectric sensor and aluminum substrate after free thermal expansion has occurred in the materials. The springs are then coupled in parallel to determine the equilibrium spring height that would occur when the force of compression on the taller spring (aluminum in our case) equals the force of elongation on the shorter spring

(piezoelectric sensor) so that their deformed lengths are equal. An equivalent spring stiffness per unit depth may then be calculated by:

$$k_i = \frac{E_i t_i d}{l_i}, \tag{22}$$

where we know $l_i \sim l_j$. The difference in spring heights is then:

$$\Delta h = \Delta l_i - \Delta l_j = \Delta x_i - \Delta x_j, \tag{23}$$

where the force equation can be written:

$$F_i = k_i \Delta x_i, \tag{24}$$

and we know from equilibrium $F_i = -F_j$. Substituting and solving for Δx_i gives:

$$\Delta x_i = \frac{\Delta h}{\left(1 + {}^{k_i}\!/\!_{k_2}\right)} = \frac{\Delta h}{\left(\dfrac{k_j + k_i}{k_j}\right)}. \tag{25}$$

The relationship between force per unit length and stress is then given by:

$$\sigma_i = \frac{F_i}{t_i} = \frac{k_i \Delta x_i}{t_i}, \tag{26}$$

which results in a stress level in the piezoelectric sensor of 53 MPa for $E_1 = 7.31 \times 10^{10}$ Pa, $E_2 = 8.40 \times 10^{10}$ Pa, $t_1 = .001$ m, $t_2 = 0.0002$ m, and $L = .01$m. This analysis ignores the axisymmetric symmetry of the sensor, the bending stresses, and transient thermal effects, which would tend to increase stress levels within the piezoelectric sensor material. For failure stress levels estimated at 70-80 MPa for the piezoelectric materials used, the possibility of fracture of the sensor is a real possibility for a +100F increase in temperature and the thermal expansion mismatch conditions present.

5. CONCLUSIONS

The long-term operability, durability, and survivability of integrated sensor systems and their associated hardware are a critical aspect of integrated systems health management (ISHM). Environmental effects due to temperature cycling, outdoor exposure, electrochemical exposure, and dynamic vibrations in particular can have a significant impact on the general performance of surface-bonded and fully-integrated sensor systems. Previous work had shown that the performance of surface-bonded piezo sensors can degrade due to environmental effects such as vibrations, temperature fluctuations, and substrate flexure motions. In this current effort, the bond and piezo material characteristics of a typical surface-bonded piezo sensor system were studied to understand and improve the long-term durability and survivability of the sensor system. Analytic models were used to understand stress-strain relationships for the bonded sensor system, with a special emphasis being place on coefficient of thermal expansion issues. The key result of this analysis described the partitioning of load between the substrate and sensor as being dependent on the relative stiffness between the two materials. Regarding the influence of the adhesive material layer, the load was found to be asymptotically transferred into the sensor from its edge interface, moving toward the center of the sensor at a rate determined by the shear modulus and thickness of the adhesive, the substrate stiffness, and the sensor thickness. For a thin piezoelectric disk bonded to an aluminum panel substrate material, an analysis of thermal expansion mismatch showed that thermal expansion and contraction of the piezo disk due to modest aircraft temperature cycling events can induce loads approaching nominal failure limits. These preliminary analytic results tend to support the previous experimental evidence for bonded sensor disbond and cracking events, and offer insight into the material properties and load transfer mechanisms which must be considered in durable surface bonded sensor applications. Future activities will focus on identifying the optimal bond

conditions and piezo material type, with the ultimate goal of improving the robustness of health monitoring systems through improved sensor system design and packaging.

ACKNOWLEDGEMENTS

The authors would like to thank Mr. Steve Martin for his help in developing analytic and computational models for the bonded piezoelectric sensor system, without which this paper would not have been possible.

REFERENCES

1. Giurgiutiu, V., Zagrai, A., and Bao, J., "Piezoelectric Wafer Embedded Active Sensors for Aging Aircraft Structural Health Monitoring, International Journal of Structural Health Monitoring, Vol. 1, 2002, pp. 41-61.
2. Dalton, R., Cawley, P., and Lowe, M., "The Potential of Guided Waves for Monitoring Large Areas of Metallic Aircraft Fuselage Structures," Journal of Nondestructive Evaluation, Vol. 20, 2001, pp. 29-45.
3. Ihn, J., and Chang, F.-K., "Build-in Diagnostics for Monitoring Crack Growth in Aircraft Structures," Proceedings of SPIE's 9th International Symposium on Smart Structures and Materials, March 2002, San Diego, CA.
4. Giurgiutiu, V., Zagrai, A., Bao, J., Redmond, J., Roach, D., and Rackow, K., "Active Sensors for Health Monitoring of Aging Aerospace Structures," International Journal of the Condition Monitoring and Diagnostic Engineering Management, Vol. 6, No. 1, 2003.
5. Blackshire, J.L., Giurgiutiu, V., Cooney, A., amd Doane, J., "Characterization of Sensor Performance and Durability for Structural Health Monitoring Systems," Proceedings of SPIE's 12th International Symposium on Smart Structures and Materials, March 2005, San Diego, CA.
6. Blackshire, J.L., and Cooney, A., "Characterization of Bonded Piezoelectric Sensor Performance and Durability in Simulated Aircraft Environments," 32nd Review of Progress in Quantitative NDE, Brunswick, ME, 2005.
7. Basheer, M., Derriso, M., and Rao, V., "Self Organizing Wireless Sensor Networks for Structural Health Monitoring," in Structural Health Monitoring 2003, Fu-Kuo Chang (Ed), pp. 1193-1207.
8. Blackshire, J., and Sathish, S., "Near-field ultrasonic scattering from surface-breaking cracks," Applied Physics Letters, Vol. 80, 2002, pp. 3442-3444.
9. Blackshire, J., "Interferometric and Holographic Imaging of Surface Wave Patterns for Characterization of Material Degradation," Nondestructive Materials Characterization with Applications to Aircraft Materials, N. Meyendorf, P. Nagy, and S. Rokhlin editors, Springer-Verlag, New York, 2003, pp. 113-140.
10. Rose, L., "Theoretical Analysis of Crack Patching," in Bonded Repair of Aircraft Structures, A. Baker and A. Jones, editors, martinus Nihoff Publishers, 1988.